CrossMark

Remote measurement of low-energy radiation based on ARM board and ZigBee wireless communication

Xu Wang[1] · Song-Ling Zhang[1] · Guo-Xiang Song[1] · De-Fei Guo[1] · Chun-Wang Ma[2] · Fang Wang[1]

Abstract We propose a system for remote measurement of low-energy radiation, which is implemented using an ARM board and a ZigBee module. The ARM STM32F103 board employs a horizontal and vertical moving CMOS camera for front-end data acquisition. The camera can detect radiation over different coordinates given by latitude and longitude in a determined area. For image processing, we used the subtraction–summation algorithm based on gradient multiplication and edge detection. Compared to algorithms such as the max grayscale value, subtraction–summation, and whole summation, the improved subtraction–summation algorithm filters noise and removes the background grayscale value of the whole image to attain higher accuracy, stronger anti-interference ability, and better consistency to determine the radiation dose. We dedicated one port of the transmission module to send data through the STM32F103 board, whereas another port is connected to the ZigBee module for data reception. By employing this architecture, we achieved low power consumption and fast response in the remote data transmission. Overall, the proposed system performs the remote measurement of low-energy radiation with stability and reliability, which is required for critical scenarios such as the remote detection of nuclear radiation.

Keywords CMOS image sensor · ARM board · Subtraction–summation algorithm · Gradient multiplication · Edge detection · ZigBee wireless transmission

✉ Chun-Wang Ma
machunwang@126.com

[1] College of Electronics and Electrical Engineering, Henan Normal University, Xinxiang 453007, China

[2] College of Physics and Materials Science, Henan Normal University, Xinxiang 453007, China

1 Introduction

In recent years, the development of nuclear radiation detection based on CMOS technology has notably increased. However, improvements are still necessary to deploy accurate remote measurement systems for low-energy radiation. In fact, the traditional CMOS radiation detection technology is limited for remote detection, as the electrophysical characteristics of the detector single crystals, CdZnTe and CdTe, and radiation monitoring of the gaseous electron multiplier muon detectors are difficult remote measurements and demand high amounts of power [1–3]. In contrast, ZigBee modules are affordable, have low power consumption, and simplify networking and remote communication, and hence, they can be suitable for remote measurement systems of low-energy radiation [4, 5]. Unlike the traditional radiation detection systems, we propose the combination of an ARM board and ZigBee wireless transmission to achieve remote measurement of low-energy radiation. Moreover, we evaluated different methods to improve the calculation of the grayscale value and developed the subtraction–summation algorithm based on gradient multiplication and edge detection. Consequently, we improved the measurement accuracy of low-energy radiation. Furthermore, the combination of ARM

technology and ZigBee communication not only allows the remote measurement of low-energy radiation, but also improves the reliability and stability of the system.

2 Experimental setup

The block diagram of the system hardware is illustrated in Fig. 1. We used the PA2 and PA3 pins from the serial port of the STM32F103 board. In the transmitter, the data (highlight positions and sum of the corresponding pixel grayscale values) are processed in MATLAB and stored in the STM32F103 board and then sent through the STM32F103 serial port 2 (pins PA2 and PA3). Specifically, for data processing, the data are transmitted through the external RS232 interface of pins PA2 and PA3. Then, the STM32F103 board and ZigBee module communicate through an interface that converts the RS232 signal into TTL communication (Tx–Rx, Rx–Tx, GND, Vcc), and the received data are stored in the ZigBee module. Finally, an LCD in the ZigBee module displays the coordinates and measurement outcomes.

2.1 Wireless transmission

By using the STM32F103 board as main controller, the acquired digital image is sent from an OV7670 camera module to the LCD [6]. In addition, the image data are processed using the proposed subtraction–summation algorithm based on gradient multiplication and edge detection. Finally, a transparent transmission module converts RS232 into TTL communication to send data.

2.2 Wireless reception

ZigBee modules feature low power consumption, strong anti-interference ability, and low cost. Moreover, in the specialized mode of low power consumption, the ZigBee communication data rate is low, which further contributes to shorten the transmission and reception time. The radiation source consists of low-energy gamma waves, so it meets the measurement requirements in the working mode. ZigBee technology is also embedded with anti-jamming

Fig. 1 System hardware diagram

characteristics that are 1000 times stronger than those of Bluetooth, WLAN, and FSK protocols and thus improves the reliability of data measurements. Furthermore, its simple protocols allow reducing the requirements for the storage and computing power in the nodes [7]. Consequently, data reception based on ZigBee technology is reliable and affordable.

3 Materials and methods

We first analyzed the max grayscale value algorithm and found that it does not contain all the pixel grayscale values of the highlights. Next, we analyzed the subtraction–summation algorithm that consists of three steps: (1) image graying; (2) background removal from the grayscale image; (3) grayscale value sum of the whole image. We found that in the subtraction process, the error to determine the background grayscale value affects the calculation accuracy and does not produce suitable outcomes.

Hence, we evaluated the whole summation algorithm that has a higher calculation accuracy compared to both the max grayscale value and the subtraction–summation algorithms. The implementation of this algorithm is detailed as follows.

(1) Image graying. According to the YUV color space, the Y component corresponds to the brightness of a pixel. The relationship between the RGB and YUV color space allows to establish a transformation from the RGB color components to the Y brightness component as

$$Y = 0.3R + 0.59G + 0.11B. \tag{1}$$

This brightness value is used as the gray value of the pixel, which is denoted as x_i.

(2) Binarization of the gray image. We considered 256 brightness levels in the gray image, and the binarization threshold was set using the MATLAB automatic threshold selection function. The resulting binary image still reflects general and local features [8]. In this step, the grayscale value corresponding to each pixel is denoted as y_i.

(3) A new image is obtained by multiplying the binary and grayscale images, and each resulting pixel value is denoted as z_i.

(4) Finally, each pixel value of the multiplied image is summed up. The sum of the pixel grayscale values for overall highlights can be determined by
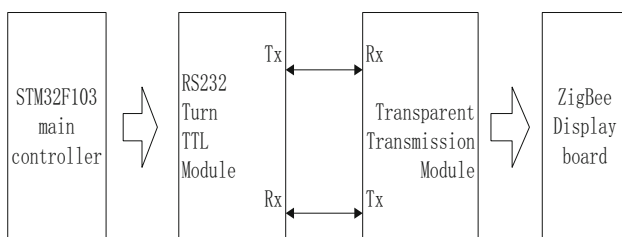
$$\text{sum} = \sum Z_i = \sum x_i y_i. \tag{2}$$

After applying this algorithm, we found that it is sensitive to noise and hence more suitable for applications having either weak or no noise.

Furthermore, the three above-mentioned algorithms have a limited anti-interference ability, and the algorithm taking an $n \times n$ square as the boundary [9] presents some accuracy errors. Thus, we used edge detection and summed the pixel grayscale values within the boundaries to introduce a method for calculating the radiation dose based on the grayscale value of the corresponding images. Traditional edge detection algorithms are based on the first derivative to improve robustness against noise, but the edge location is not accurate. In contrast, other edge detection algorithms based on the second derivative results in high accuracy, but they are sensitive to noise. Hence, we propose a method based on gradient multiplication for edge detection. This method suitably and accurately locates the edges and is robust against noise, and the resulting detection provides more complete edges than traditional algorithms. We first employed the whole summation algorithm based on gradient multiplication and edge detection to improve the calculation method of the binarization threshold. For this method, the background grayscale value is determined using the following process: (1) determine the image gradient map using the Sobel operator; (2) determine the image gradient map using the Laplacian operator; (3) multiply the two maps to obtain another gradient map; (4) the image obtained from the new gradient map is binarized and then used as mask image; (5) determine the background grayscale value by obtaining the average grayscale value of the edge pixels. The mask image in the fourth step and the original image were multiplied to obtain an image that only retains the grayscale values of edge pixels. The sum of the grayscale values in this image and the mask image are denoted by P and Q, respectively. Thus, the background grayscale value is given by $B = P/Q$, which is considered as the binarization threshold. This threshold mitigates the error related to that from the original whole summation algorithm and improves the anti-interference ability and consequently the stability of the system.

However, this algorithm does not remove the background grayscale value and thus generates error in determining the radiation dose. To solve this problem, we propose using the subtraction–summation algorithm based on gradient multiplication and edge detection. This algorithm improves the method for determining the background grayscale value in the second step of the above-mentioned subtraction–summation algorithm. In fact, for this improved algorithm, we use the background grayscale

value obtained from the whole summation algorithm based on gradient multiplication and edge detection. Consequently, we obtained higher accuracy, better consistency to determine the radiation dose, stronger anti-interference ability, and easier operation if compared to all the other algorithms mentioned in this section. Hence, we used the subtraction–summation algorithm based on gradient multiplication and edge detection to implement the proposed system.

4 Results and discussion

4.1 Analysis of radiation image algorithms

Compared with both the max grayscale value and the subtraction–summation algorithms, the whole summation algorithm features characteristics such as high speed, accurate positioning, low error, and simple operation. First, the grayscale image is obtained by applying image graying. Next, the binary image is obtained from the gray image. Finally, another image is obtained by multiplying the binary and grayscale images. In the original image, the bright spot cannot be clearly observed, whereas it is clearly visible after the image processing. A three-dimensional view of the image pixels can help to better visualize the location of the bright spot. The grayscale image before processing is shown in Fig. 2a, whereas the corresponding result after applying the whole summation algorithm is shown in Fig. 2b. When the CMOS image sensor acquires an image, a γ photon usually hits several neighboring pixels and forms an irregular shape and hence causes an error in the max grayscale value algorithm. However, the
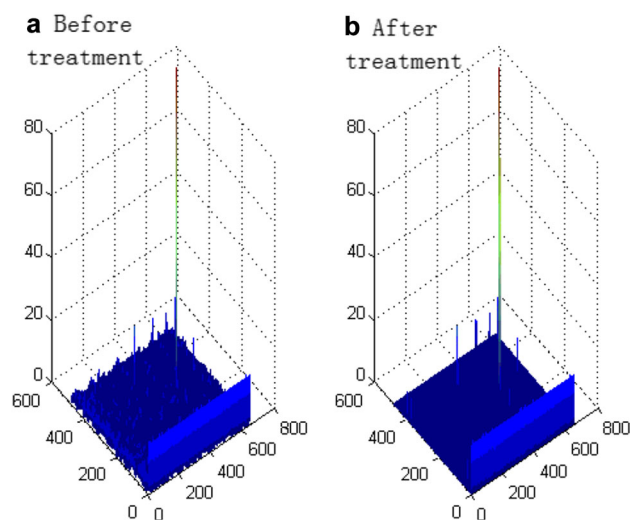

Fig. 2 (Color online) Three-dimensional pixel intensity image corresponding to the radiation image of ^{60}Co. **a** Original radiation image of ^{60}Co. **b** Image processed using the whole summation algorithm

whole summation algorithm can consider the grayscale value of the whole photon, thus avoiding leakage and improving the measurement accuracy.

We also compared the image processing capabilities between the max grayscale value, subtraction–summation, and whole summation algorithms. For this comparison, we applied the algorithms to the radiation image of the same cobalt source acquired over 9 consecutive frames. The normalized grayscale values for the images are shown in Table 1. A fourth-degree polynomial curve fitting was used in the data of Table 1, whose results are shown in Fig. 3. The curves clearly describe the variation of radiation dose over time. In addition, it is clear that the curve corresponding to the max grayscale value algorithm is very wide, which indicates a high sensitivity and causes a poor anti-interference ability. In contrast, the curve corresponding to the subtraction–summation algorithm is very narrow, which indicates a low sensitivity and a difficulty to detect small changes in radiation dose. Finally, the curve corresponding to the whole summation algorithm lies between those of the two other algorithms. Thus, this algorithm can detect small changes and has a suitable anti-interference ability in the presence of either weak or no noise.

Given the limited anti-interference ability of the whole summation algorithm, we used the subtraction–summation algorithm based on gradient multiplication and edge detection. To verify this method, we processed the same image using the original and improved versions of both the subtraction–summation and whole summation algorithms. The corresponding background grayscale value and the binarization threshold are listed in Table 2.

Next, we processed the radiation detection images of the same cobalt source acquired over 9 consecutive frames using the subtraction–summation and whole summation algorithms, both based on gradient multiplication and edge detection. The original and min–max normalization data of the cobalt source radiation are listed in Table 3, and we employed a fourth-degree polynomial curve fitting for the normalized data in Table 3, which is shown in Fig. 4. From the graph, we can see that the amplitude obtained from the subtraction–summation algorithm is higher than that obtained from the whole summation algorithm. Moreover, this amplitude shows an increasing value over time, which
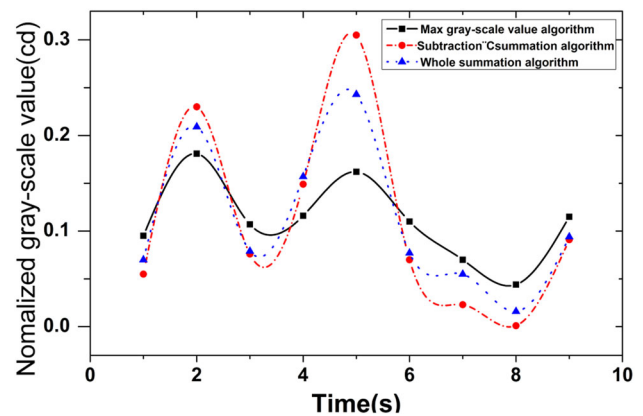

Fig. 3 (Color online) Curve for the data in Table 1

is consistent with the change in radiation dose. In addition, the subtraction–summation algorithm shows higher precision and robustness against noise. Furthermore, it suitably meets the design requirements of the ZigBee-based hardware and can retrieve more stable and reliable measurement data for the system.

4.2 Hardware tests

Design and applications based on ARM, ZigBee, and smart phone architectures are currently widespread. For instance, there is research on robot vision based on ARM and digital signal processing to develop an assistant robot for elderly and disabled individuals [10], as well as the design and implementation of a gray LED controller based on ARM architecture and FPGAs [11]. Other developments include a ZigBee and Bluetooth protocol converter based on a multi-sinks wireless sensor network [12], a ubiquitous healthcare service using ZigBee and smart phones for elderly patients [13], and an application to survey surrounding ionizing radiations with a smart phone that provides low cost and convenience for the general public [14]. However, research on the combination of ARM and ZigBee technologies for remote measurements is scarce. Thus, we propose a system for remote measurement of low-energy radiation by combining ZigBee wireless transmission and ARM data processing.

To guarantee accuracy of data transmission and reception, we first established the corresponding parameters

Table 1 Normalized grayscale value of a ^{60}Co source over consecutive frames

Algorithm	Image 1	Image 2	Image 3	Image 4	Image 5	Image 6	Image 7	Image 8	Image 9
Max grayscale value algorithm	0.095	0.181	0.107	0.116	0.162	0.110	0.070	0.044	0.115
Subtraction–summation algorithm	0.055	0.230	0.076	0.149	0.305	0.070	0.023	0.001	0.091
Whole summation algorithm	0.070	0.209	0.079	0.157	0.243	0.077	0.055	0.016	0.094

Table 2 Background grayscale value and binarization threshold of the original and improved versions of the subtraction–summation and whole summation algorithms

Parameter (algorithm)	Original algorithm	Improved algorithm
Binarization threshold (whole summation algorithm)	6.018	3.152
Background grayscale value (subtraction–summation algorithm)	3	3.152

Table 3 Original and normalized data of a ^{60}Co source radiation over consecutive frames

Algorithm	Image 1	Image 2	Image 3	Image 4	Image 5	Image 6	Image 7	Image 8	Image 9
Improved subtraction–summation algorithm	14,788	7533	14,798	11,488	12,452	14,137	13,680	13,975	16,506
Min–max normalization	0.809	0.000	0.810	0.441	0.548	0.736	0.685	0.718	1.000
Improved whole summation algorithm	25,822	13,819	25,805	23,488	27,244	23,041	35,529	41,338	30,186
Min–max normalization	0.436	0.000	0.436	0.351	0.488	0.335	0.789	1.000	0.595
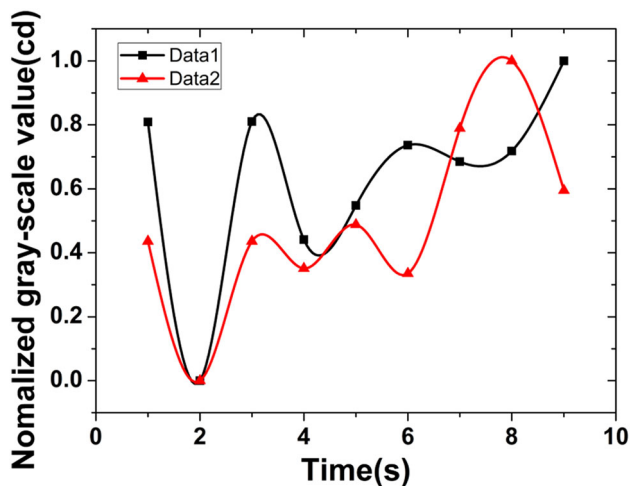
Fig. 4 (Color online) Curve for the data in Table 3 (Data 1 and Data 2 represent the normalized data from the subtraction–summation and the whole summation algorithms, respectively. Both algorithms were based on gradient multiplication and edge detection)

(e.g., baud rate, parity bit, and data bits). Considering the coordination between modules, we set a 9600 baud rate and even parity. The received data are stored in the ZigBee module, and at this receiving end, we display data on the LCD corresponding to the coordinates and summation results. The results listed in Table 4 clearly show that the combination of the ARM STM32F103 board and ZigBee communication allows to be achieved stable and reliable remote data transmission. Furthermore, ZigBee provides a strong anti-jamming performance in low signal-to-noise ratio (SNR) environments, which is 1000 times higher than that of Bluetooth, WLAN, and FSK. In fact, experimental results show that the symbol error rate (SER) resulting from the ZigBee protocol with a SNR of 4 dB can reach 10^{-9}. To achieve the same SER, the SNR of the Bluetooth protocol should be of 16 dB and that of the WLAN 802.11b protocol should be of 10 dB. By using the ZigBee module, the system not only performs remote measurements, but also ensures data transmission without distortion. Moreover, the remote measurement of low-energy radiation can be stably realized by combining ARM and ZigBee architectures.

Table 4 Hardware test for the system combining ARM and ZigBee technologies

Data	1	2	3	4	5	6	7	8	9	10
Sending end	(86;50)	(24;92)	(40;51)	(124;204)	(159;44)	(80;211)	(213;116)	(162;11)	(63;43)	(103;204)
Position coordinate (H;L) Sum result	14,788	7533	14,798	11,488	12,452	14,137	13,680	13,975	16,506	25,822
Receiving end	(86;50)	(24;90)	(40;51)	(124;204)	(159;44)	(80;211)	(213;116)	(162;11)	(63;43)	(103;204)
Position coordinate (H;L) Sum result	14,788	7533	14,798	11,488	12,452	14,146	13,680	13,975	16,506	25,822

5 Summary

We designed and implemented a remote radiation-detection system based on an ARM board and a ZigBee module. In addition, we verified that the subtraction–summation algorithm based on gradient multiplication and edge detection improves the measurement accuracy. Then, we combined the data processing capabilities of the ARM STM32F103 board and the remote transmission function of the ZigBee module to perform remote data transmission of undistorted measurements of gamma waves irradiated from a cobalt source. The experimental results verified the effectiveness of employing the proposed algorithm and the feasibility of the system that combines ARM and ZigBee architectures. Furthermore, the system can be used for accurate and stable remote measurements to monitor low-energy radiation.

References

1. I.M. Gazizov, A.A. Smirnov, V.G. Fedorkov et al., Uncooled CdTe and CdZnTe based detectors for γ-Radiation spectrometry. Atom. Energy **121**, 65–370 (2017). https://doi.org/10.1007/s10512-017-0213-4
2. B. Manuela, B. Helmut, S. Michael, Machine detector interface studies: layout and synchrotron radiation estimate in the future circular collider interaction region. Phys. Rev. Accel. Beams **20**, 011008 (2017). https://doi.org/10.1103/PhysRevAccelBeams.20.011008
3. L. Dimitrov, P. Iaydjiev, G. Mitev et al., Radiation monitoring of the GEM muon detectors at CMS. Phys. Part. Nuclei Lett **13**, 551–556 (2016). https://doi.org/10.1134/S1547477116050174
4. T. Mitsugu, Application of ZigBee sensor network to data acquisition and monitoring. Meas. Sci. Rev. 9, 183–186(2009). doi: http://www.measurement.sk/2009/S1/Terada.pdf
5. L.K. Wadhwaa, R.S. Deshpandea, V. Priyeb, Extended shortcut tree routing for ZigBee based wireless sensor network. Ad Hoc Netw. **37**, 295–300 (2016). https://doi.org/10.1016/j.adhoc.2015.08.025
6. Q.Q. Cheng, Y.Z. Yuan, C.W. Ma et al., Gamma measurement based on CMOS sensor and ARM microcontroller. Nucl. Sci. Tech. **28**, 122 (2017). https://doi.org/10.1007/s41365-017-0276-x
7. H.F. Wang, Environmental monitoring system based on ZigBee wireless sensor and low-power technology. Adv. Mater. Res. **662**, 701–704 (2013). https://doi.org/10.4028/www.scientific.net/AMR.662.701
8. S. Yuan, G.Y. Zhang, J.H. Wu et al., Study of license plate recognition technology. Adv. Mater. Res. **834–836**, 1035–1038 (2014). https://doi.org/10.4028/www.scientific.net/AMR.834-836.1035
9. F. Wang, M.Y. Wang, Y.F. Liu et al., Obtaining low energy γ dose with CMOS sensors. Nucl. Sci. Tech. **25**, 060401 (2014). https://doi.org/10.13538/j.1001-8042/nst.25.060401
10. C.Z. Wang, X.D. Zhang, X.Z. Wu, Research on robot vision technology based on ARM and DSP for age and disabled helping robot. Key Eng. Mater. (2010). https://doi.org/10.4028/www.scientific.net/KEM.455.42
11. X.M. Liu, S.H. Zheng, The design and realization of gray LED controller based on ARM + FPGA. Adv. Mater. Res. (2012). https://doi.org/10.4028/www.scientific.net/AMR.433-440.4640
12. C. Guo, Y. Zhou, Q. Ye et al., A Zigbee and bluetooth protocol converter based on multi-sinks wireless sensor network. J. Netw. **9**, 1854–1860 (2014). https://doi.org/10.4304/jnw.9.7.1854-1860
13. H.J. Lee, S.H. Lee, K.S. Ha et al., Ubiquitous healthcare service using Zigbee and mobile phone for elderly patients. Int. J. Med. Inform. **78**, 193–198 (2009). https://doi.org/10.1016/j.ijmedinf.2008.07.005
14. Q.Y. Wei, R. Bai, Z.P. Wang et al., Surveying ionizing radiations in real time using a smartphone. Nucl. Sci. Tech. **28**, 70 (2017). https://doi.org/10.1007/s41365-017-0215-x